

Directionality is an inherent property of biochemical networks

Feng Yang,* Feng Qi, and Daniel A. Beard†

Biotechnology and Bioengineering Center, Department of Physiology,

Medical College of Wisconsin, Milwaukee, Wisconsin 53226, USA

(Dated: September 18, 2018)

Abstract

Thermodynamic constraints on reactions directions are inherent in the structure of a given biochemical network. However, concrete procedures for determining feasible reaction directions for large-scale metabolic networks are not well established. This work introduces a systematic approach to compute reaction directions, which are constrained by mass balance and thermodynamics, for genome-scale networks. In addition, it is shown that the nonconvex solution space constrained by physicochemical constraints can be approximated by a set of linearized subspaces in which mass and thermodynamic balance are guaranteed. The developed methodology can be used to *ab initio* predict reaction directions of genome-scale networks based solely on the network stoichiometry.

PACS numbers: 89.65.-s, 89.75.Hc, 87.23.Ge, 87.23.Kg

*Electronic address: fyang@mcw.edu

†Electronic address: dbeard@mcw.edu

Constraint-based approaches to analyzing biochemical networks, such as flux balance analysis (FBA) and energy balance analysis (EBA), have found widespread applications in system analysis of metabolic networks [1]. A successful set of procedures has been established for determining metabolic reactions which are present in a genome-scale system [2, 3]. However, the procedure for determining feasible reaction directions is less concrete and arbitrary to some degree [4, 5]. Yet the information on reaction directions is crucial to ensure that predicted reaction fluxes are physically feasible and obtained results are physiologically reasonable [6, 7].

Allowable reaction directions in a biochemical network are constrained by mass-conservation constraints and thermodynamic constraints, both arising from the stoichiometry of a given network [5, 6, 8, 9]. While the linear mass-conservation constraint is rigorously applied in many applications, the nonlinear thermodynamic constraint is not typically considered due to its implicit nonlinearity and NP-completeness of the associated problems. Consequently, the flux distribution determined solely by the principle of mass-conservation, may not be physically feasible.

The nonlinear thermodynamic constraint is based on the second law of thermodynamics which requires that each internal reaction with non-zero flux must dissipate energy [7]. For a set of reaction directions to be thermodynamically feasible (T-feasible), there must exist a thermodynamic driving force for the reaction directions on a given network. A robust algorithm to implement this constraint, which is based on an NP-complete computation of entire elementary modes for a network, has been previously developed [10]. However, an appropriate method for genome-scale networks has not been developed until now. Here, we introduce a new methodology for systematically determining feasible reaction directions for large-scale networks and apply it to a biochemical network model of the mammalian cardiomyocyte [11].

To illustrate mass-balanced and thermodynamically-defined determination of feasible reaction directions, an example network illustrated in Fig. 1 is used. In this network, transport fluxes J_1 , J_{12} , and J_{13} are assumed to have net flux in the direction indicated by the arrows in the figure (defined as positive). In general, we assume that some subset of reaction fluxes (typically transport fluxes) have associated with them prior assigned directions. A set of these predefined constraints is denoted as Ψ . For example of Fig. 1, the constraints on boundary fluxes can be expressed Ψ : $\text{sign}(J_1, J_{12}, J_{13}) = \{+, +, +\}$.

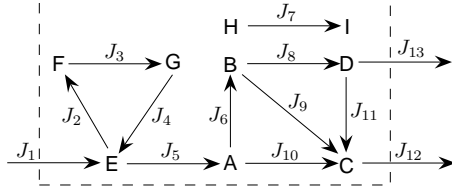


FIG. 1: A example network composed of 13 reactions (J_{1-13}) and 9 species (A through I). J_1 , J_{12} and J_{13} are transport (boundary) fluxes that transport mass into and out of the system; J_2 through J_{11} are internal fluxes, as shown in the dashed box.

Flux directions constrained by mass-balance only For a flux vector \vec{J} to be feasible, steady-state mass balance requires

$$\sum_j S_{ij} \cdot J_j = 0, \text{ and } \vec{J} \text{ obeys } \Psi \quad (1)$$

where S_{ij} is the stoichiometric coefficient of metabolite i and reaction j . *Mass-irreversible (MI)* fluxes are those fluxes, the signs of which are specified by considering the mass-balance and boundary constraints of Eq. 1 alone. For example of Fig. 1, J_5 is mass-irreversible, because there exists no feasible flux vector \vec{J} that satisfies Eq. 1 for which $J_5 < 0$. In fact, here we say flux J_5 is *strictly mass-irreversible (sMI)* because $J_5 > 0$ and the equality $J_5 = 0$ is not feasible for finite boundary flux values. Such fluxes represent the backbone of the network; without them, the network would not function with any nonzero fluxes. In addition, J_7 is characterized as *mass-infeasible (MN)* because no flux is possible for this network given the boundary conditions and the network stoichiometry. The remaining internal reactions in Fig. 1 (J_{2-4} , J_6 , and J_{8-11}) are denoted as *mass-reversible (MR)*.

Flux directions constrained by thermodynamic constraints The nonlinear thermodynamic constraint requires that there exists a driving force $\vec{\mu}$ for a given flux vector \vec{J} such that

$$\begin{aligned} \Delta\mu_j &= \sum_i \mu_i \cdot S_{ij}, \quad J_j \cdot \Delta\mu_j \leq 0, \\ \text{and } J_j &= 0 \text{ if and only if } \Delta\mu_j = 0, \end{aligned} \quad (2)$$

where i and j are the indexes for a particular metabolite and internal reaction, respectively. *Thermodynamically irreversible (TI)* fluxes are those identified as mass-reversible by Eq. 1 but found to be irreversible when T-constraints (Eq. 2) is imposed. In Fig. 1, J_6 , J_8 and

J_{10} are *TI* fluxes, with their feasible net fluxes in the positive directions illustrated in the figure. There exists no T-feasible flux patterns for which these reactions operate with net fluxes in the negative direction. In addition, reactions J_2 , J_3 and J_4 are characterized as *T-infeasible (TN)* because no net flux is possible in any of flux directions; reactions J_9 and J_{11} can proceed in both directions while still satisfying mass-balance and T-constraints, and thus they are denoted as *T-reversible (TR)* reactions. An algorithm for determining *TI*, *TN*, and *TR* fluxes in a given network is presented in the Supplemental Material.

In characterizing the impacts of applying T-constraints, we observe that a mass-reversible (*MR*) reaction is potentially *reducible* by T-constraints, either reduced as T-irreversible (*TI*) or reduced as T-infeasible (*TN*). In addition, a mass-irreversible (*MI*) reaction is also *reducible* if it is later characterized as T-infeasible, though it may not be necessarily true. Furthermore, the constraints of Eq. 2 can be equivalently represented by the orthogonality of a flux vector \vec{J} against the sign patterns of the exhaustive set of infeasible reaction cycles [7]. Here, a *reaction cycle* is a set of reactions, the summation of which results in cancellation of all participating metabolites. There are 4 reaction cycles imbedded in the example network (Fig. 1), for example, three fluxes of J_2 , J_3 , and J_4 make up a cycle: $J_2 : E \rightleftharpoons F; J_3 : F \rightleftharpoons G; J_4 : G \rightleftharpoons E$, and thus $J_2 + J_3 + J_4 : \emptyset = \emptyset$.

Flux directions that are sufficient for T-feasibility The overall goal of *ab initio* prediction is to generate a set of irreversibility constraints that guarantees the T-feasibility. However, the constraints defined so far (*MI* and *TI*) are merely necessary, but not sufficient to ensure the T-feasibility in general [10]. Consequently, the solution space defined by *MI* and *TI* is not linearly constrained and still a nonconvex space. For instance, to generate a linearly constrained, T-feasible solution space for the example network, one of the following additional linear constraints has to be included: I) If $J_9 > 0$, then J_{11} is feasible in any directions; II) If $J_{11} < 0$, then J_9 is feasible in any directions; III) If $J_9 < 0$ and $J_{11} < 0$; IV) If $J_9 > 0$ and $J_{11} > 0$, *etc.* The resulting convex spaces (${}_lEBA$), as well as traditional flux balance space (*FBA*) and nonconvex T-feasible space(${}_fEBA$), are illustrated in Fig. 2.

In general, in addition to those necessary conditions we need to determine a set of extra irreversibility constraints (*EI*) to guarantee the T-feasibility. The resulting linearized solution spaces (${}_lEBA$) defined by *MI*, *TI*, and *EI* are subsets of the nonconvex T-feasible space (${}_fEBA$). However, a complete enumeration of these subspaces is not practicable (maximally 21^n , where n is the number of T-reversible fluxes in a given network), especially

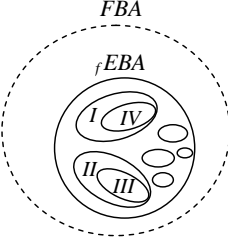


FIG. 2: Illustration of the solution space constrained by mass-balance only (*FBA*), the space constrained by additional nonlinear T-constraints (*fEBA*), and the linearized T-feasible spaces (*lEBA*, such as the solution spaces of I, II, III, IV, *etc*). The space defined by traditional *FBA* may not be physically feasible; the space of *fEBA*, in which both mass-balance and energy-balance are guaranteed, represents a better approximation of network behaviors than using *FBA* only.

for large-scale networks. To approximate the nonconvex *fEBA* space, however, it is possible to enumerate a limited set of subspaces (*lEBA*) in which the number of reversible reactions is maximized. The subspaces obtained represent the largest subsets of *fEBA*, such as the spaces of I and II in Fig. 2. Therefore, the network behaviors could be maximally captured by studying these linearized subspaces. For those subspaces that are heavily constrained, for instance, the spaces of III, IV and many others, it is assumed that they represent the non-typical network behaviors, or the time staying in these states is highly limited. In practice, determining which set of *lEBA* subspaces for particular studies may require further constraints or evidences from experimental observations.

In summary, for a given network with associated prior reaction directions, to generate a convex, T-feasible solution space, reaction directions can be categorized as {MN, sMI, MI, TN, TI, TR, and EI}. A diagram which shows their relationship are illustrated in Fig. 3. In particular, when all reaction directions other than those of predefined boundary fluxes are assumed reversible, a few theorems have been observed in the above analysis.

Theorem 1 Mass-irreversible reactions are not reducible by thermodynamic constraints. Suppose a *MI* reaction that connects species A to B, $A \rightarrow B$, is reduced as T-infeasible by a reaction loop which connects species B to A along *L*, $B \rightarrow^L \rightarrow A$. As a result, there must be a pathway that connects A to B along a reversed loop of *L*, $A \rightarrow^{-L} \rightarrow B$, by the definition of mass balance. The existence of such a reversed loop thus disables the reducibility of the loop *L*, and there is no cycle existing between species A and B. This theorem implies a mass-irreversible reaction does not participate in any reaction

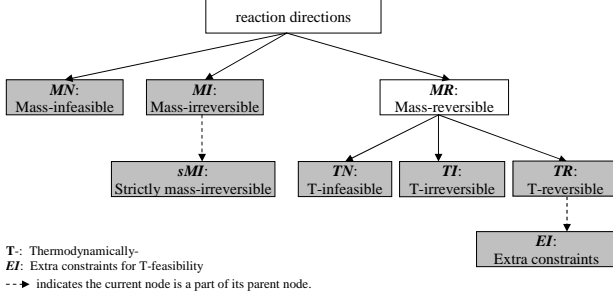


FIG. 3: Illustration of the categories of reaction directions (shaded in gray) when both mass-conservation and T-constraints are imposed.

cycle; if involved, then it must be characterized as mass-reversible by Eq. 1. In other words, $MI \cap TI = \emptyset$, where MI and TI represent the sets of mass-irreversible and T-irreversible reactions, respectively.

Theorem 2 Mass-reversible reactions can be reduced as T-irreversible or T-infeasible. Supposing a reversible flux J_i , $A \rightleftharpoons B$, involved in a loop L , then all reactions in this loop L must be reversible because of the connectivity between A and B along L . To block this reaction cycle, any reversible reactions can be chosen and reduced as irreversible. Therefore, the loop constraint is active with respect to the reversible flux J_i , which can be reduced as T-infeasible (such as J_{2-4}), or reduced as T-irreversible (such as $J_{6,8,10}$ in the example network).

Theorem 3 A reaction cycle in which all reactions are irreversible is impossible. Suppose there is a reaction cycle which contains an irreversible reaction $A \rightarrow B$, and a set of irreversible reactions along loop L , then the reactions along loop L must be reversible by mass-balance. Therefore, a fully directed cycle is impossible and any cycles can always be eliminated by assigning directions to some T-reversible reactions in the network.

The developed methodology has been applied for the metabolic network of mammalian cardiomyocyte [11] which accounts for 240 metabolites and 257 reactions. While the stoichiometric structure of this model has been adopted, the flux directions previously assigned are typically not considered. Instead, we define a network in which the directions of all boundary fluxes and two internal fluxes (ATP hydrolysis and a transport flux of $12DGrt2$), are assigned based on the published model [11], but all other reactions are assumed to be reversible in default. In this network model, three transport fluxes are constrained to operate in the direction of net uptake of substrates (glucose, oleate and oxygen) and 28 transport

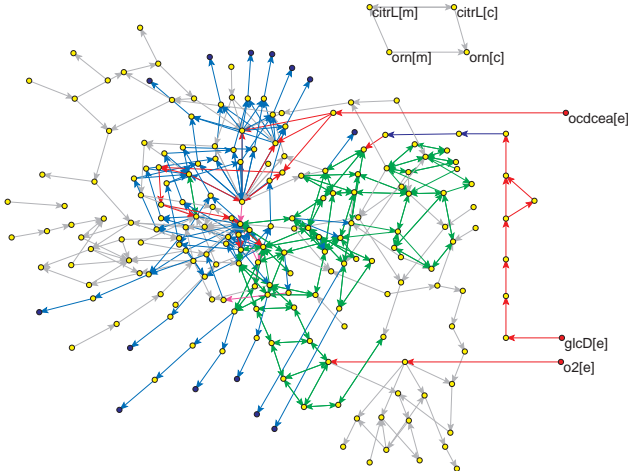
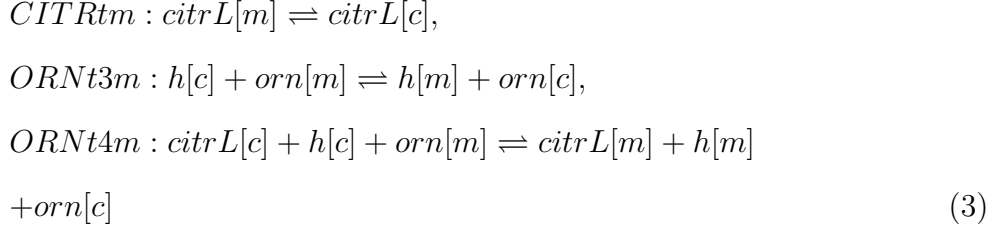


FIG. 4: Illustration of a thermodynamically feasible network of the cardiomyocyte network. The nodes and edges represent metabolites and reactions, respectively. In particular, the red, blue and yellow nodes represent the sources, the sinks and the intermediate metabolites of the network, respectively. Red edges and blue edges represent the strictly mass-irreversible reactions, and violet red edges and navy blue edges represent mass-irreversible reactions. In particular, reactions in red or violet red proceed in the same direction as the original definition of the network [11]; reactions in blue and navy blue proceed in a reversed direction. An infeasible reaction cycle is shown at the right top corner of Fig. 4. For simplicity, the currency of the biochemical networks, such as ATP, ADP, Pi, NADH, NAD, H^+ , H_2O and CO_2 , have not been shown.

fluxes (including citrate, acetate and 26 additional output fluxes) are constrained to operate in the direction of net production of reactants. A total of 33 irreversibility constraints are specified and the directions of the remaining 217 internal reactions are computed.

Given finite uptakes of glucose, oleate and oxygen, mass-balance analysis identifies 18 *sMI* internal fluxes (see red and blue fluxes in Fig. 4), which represent a set of reactions essential for this network. It also shows that only 14 products (of 32 desired metabolites) could be possibly produced from the sources (i.e. glucose, oleate, and O_2), with the aids of three reversible transport fluxes of CO_2 , H^+ , and H_2O . In addition, 70 mass-infeasible fluxes, 73 mass-irreversible fluxes, and 74 mass-reversible fluxes are found. Furthermore, the results of intensively sampled T-feasible networks (559,518,687 samples) further indicate that among 74 mass-reversible fluxes, three fluxes (*CITRtm*, *ORNt3m*, *ORNt4m*) are

T-infeasible, because these three reactions



develop a reaction cycle as $CITRtm + ORNt4m - RNt3m = \emptyset$. It is also found that $h[c]$ is the only metabolite that connects this reaction cycle to the remaining part of the network, which reminds of the reaction cycle $J_2 \rightarrow J_3 \rightarrow J_4 \rightarrow J_2$ in the example network. Thus, neither direction is feasible for all these three reactions.

The solution space defined by $MI \cup TI$ needs to be further refined since 1099 cycles are still embedded in this network. However, by specifying only 14 reversible fluxes (out of 71 T-reversible fluxes) be irreversible, it is possible to eliminate all those cycles. A final T-feasible network for mammalian cardiomyocyte has been illustrated in Fig. 4, which consists of 112 infeasible reactions, 101 irreversible reactions and 44 reversible reactions. However, such a linearly constrained subspace is not unique, as indicated in the example network. To further explore the nonlinear T-feasible space, a large number of subspaces (see Fig. 5) have been generated by assigning directions to those T-reversible fluxes. Importantly, each irreversibility assignment is generated in such a way that the maximum number of reaction cycles can be eliminated. Therefore, the generated set of linear constraints defines a feasible solution space which requires a minimal number of irreversibility constraints, and thus represents the largest linear subspace in Fig. 2.

Surprisingly, the computed T-feasible irreversibility constraints show significant difference when compared to the originally assigned directions, by which the space defined is not thermodynamically feasible (7 reaction cycles are included). To make it physically feasible, three mass-reversible fluxes ($CITRtm$, $ORNt3m$, $ORNt4m$) have to be eliminated, and at least one additional direction assignment, either specifying $AKGMALtm$ (previously assigned as reversible) be positive or specifying $ASPTAm$ be negative, has to be incorporated into the original definition of the network. Although these additional constraints do not invoke significant impacts on the overall results from [11], they do change the flux distribution with the given boundary fluxes. While the revised network represents a special subset of

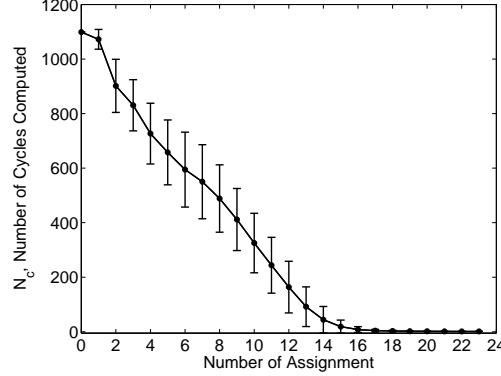


FIG. 5: Demonstration of reductions in the number of reaction cycles with extra irreversibility constraints (*EI*). It represents the results of 10^5 independent simulations for generating T-feasible solution spaces. Bars represent the standard deviation of the number of cycles that are eliminated at each particular assignment.

TABLE I: Comparison of a T-feasible network with high flexibility to the original network as well as its corresponding mass-balanced and thermodynamically balanced networks.

| | PI | PI+FBA | PI+FBA+EBA | EBA ^a |
|------------------------------|-----|--------|------------|------------------|
| Infeasible fluxes | 0 | 149 | 149 | 112 |
| Positive ^b fluxes | 156 | 60 | 61 | 42 |
| Negative ^b fluxes | 3 | 21 | 21 | 59 |
| Reversible fluxes | 98 | 27 | 26 | 44 |

^aA T-feasible network corresponds to the network shown in Fig. 4.

^bThe positive reaction direction is defined based on the left-to-right reaction direction in the original model definitions [11].

the T-feasible solution space, it is significantly different from the network which shows the maximum level of flexibility (i.e. containing the maximum number of reversible reactions). Table 1 shows the difference between an example of the largest T-feasible subspaces, and the original definition of the network (PI) and its mass-balanced network (PI+FBA) and thermodynamically balanced network (PI+FBA+EBA). The significant difference between the *ab initio* prediction and the previously assigned directions, can be explained by the fact that mass-conservation and thermodynamic constraints are by far not the only constraints that a given network must satisfy. Those nonidentified may come from gene regulatory

constraints, topological constraints, environmental constraints [12], and constraints that are accumulated from evolution and natural selection. By systematically studying the difference between the results from *ab initio* predictions and experimental observations, we may find some interesting knowledge “gap”, leading to more accurate predictions on the flux distributions.

In summary, a biophysical constraint is applied to genome-scale biochemical networks for computing flux directions and determining a linearly constrained, mass- and thermodynamically-balanced solution space. Given a reaction network and a set of prior constraints on certain flux directions (such as known transport flux directions) the algorithm determines a minimal set of irreversibility constraints (reactions directions) that is sufficient to guarantee T-feasibility. The developed methods could be used as a tool to systematically design a biochemical network, greatly facilitate the further flux balance analysis and energy balance analysis, improve their predictions of the flux distribution, and help capturing the physically meaningful behavior of the network studied. Numerically, a linear solution space will make related optimizations more reliable and efficient.

Acknowledgments

I wish to acknowledge the support of all authors, although Daniel A. Beard does not like the overall organization of this manuscript.

- [1] A. R. Joyce and B. O. Palsson. The model organism as a system: integrating 'omics' data sets. *Nat Rev Mol Cell Biol*, 7:198–210, 2006.
- [2] J. Forster, I. Famili, P. Fu, B. O. Palsson, and J. Nielsen. Genome-scale reconstruction of the *saccharomyces cerevisiae* metabolic network. *Genome Res*, 13:244–53, 2003.
- [3] C. Francke, R. J. Siezen, and B. Teusink. Reconstructing the metabolic network of a bacterium from its genome. *Trends Microbiol*, 13:550–8, 2005.
- [4] Kummel. A, Panke. S, and Heinemann. M. Systematic assignment of thermodynamic constraints in metabolic network models. *BMC Bioinformatics*, 7:512–, 2006.
- [5] N. D. Price, I. Thiele, and B. O. Palsson. Candidate states of *helicobacter pylori*'s genome-

scale metabolic network upon application of. 2006.

- [6] D. A. Beard, S. D. Liang, and H. Qian. Energy balance for analysis of complex metabolic networks. *Biophys J*, 83:79–86, 2002.
- [7] D. A. Beard, E. Babson, E. Curtis, and H. Qian. Thermodynamic constraints for biochemical networks. *J Theor Biol*, 228:327–33, 2004.
- [8] J. M. Lee, E. P. Gianchandani, and J. A. Papin. Flux balance analysis in the era of metabolomics. *Brief Bioinform*, 7:140–50, 2006.
- [9] C. S. Henry, M. D. Jankowski, L. J. Broadbelt, and V. Hatzimanikatis. Genome-scale thermodynamic analysis of escherichia coli metabolism. *Biophys J*, 90:1453–61, 2006.
- [10] F. Yang, H. Qian, and D. A. Beard. Ab initio prediction of thermodynamically feasible reaction directions from biochemical network stoichiometry. *Metab Eng*, 7:251–9, 2005.
- [11] T. D. Vo and B. O. Palsson. Isotopomer analysis of myocardial substrate metabolism: A systems biology approach. *Biotechnol Bioeng*, 2006.
- [12] B. O. Palsson. *System Biology*. Cambridge University Press, 2006.

Directionality is an inherent property of biochemical networks

Feng Yang, Feng Qi, and Daniel A. Beard*
*Biotechnology and Bioengineering Center, Department of Physiology,
 Medical College of Wisconsin, Milwaukee, Wisconsin 53226, USA*
 (Dated: September 18, 2018)

Thermodynamic constraints on reactions direct the overall behavior of a biochemical network. However, concrete procedures for determining reaction directions in large-scale metabolic networks are not well established. In this paper, we show that it is possible to compute reaction directions, which are consistent with thermodynamic constraints, for genome-scale networks. In addition, it is shown that physicochemical constraints can be approximated by thermodynamic constraints, and thermodynamic balance is guaranteed. The proposed method can predict reaction directions of genome-scale networks.

PACS numbers: 89.65.-s, 89.75.Hc, 87.23.Ge, 87.23.I

Constraint-based approaches to analyzing biochemical networks, such as flux balance analysis (FBA) and energy balance analysis (EBA), have found widespread applications in system analysis of metabolic networks [?]. A successful set of procedures has been established for determining metabolic reactions which are present in a genome-scale system [? ?]. However, the procedure for determining feasible reaction directions is less concrete and arbitrary to some degree [? ?]. Yet the information on reaction directions is crucial to ensure that predicted reaction fluxes are physically feasible and obtained results are physiologically reasonable [? ?].

Allowable reaction directions in a biochemical network are constrained by mass-conservation constraints and thermodynamic constraints, both arising from the stoichiometry of a given network [? ? ? ?]. While the linear mass-conservation constraint is rigorously applied in many applications, the nonlinear thermodynamic constraint is not typically considered due to its implicit nonlinearity and NP-completeness of the associated problems. Consequently, the flux distribution determined solely by the principle of mass-conservation, may not be physically feasible.

The nonlinear thermodynamic constraint is based on the second law of thermodynamics which requires that each internal reaction with non-zero flux must dissipate energy [?]. For a set of reaction directions to be thermodynamically feasible (T-feasible), there must exist a thermodynamic driving force for the reaction directions on a given network. A robust algorithm to implement this constraint, which is based on an NP-complete computation of entire elementary modes for a network, has been previously developed [?]. However, an appropriate method for genome-scale networks has not been developed until now. Here, we introduce a new methodology for systematically determining feasible reaction directions for large-scale networks and apply it to a bio-

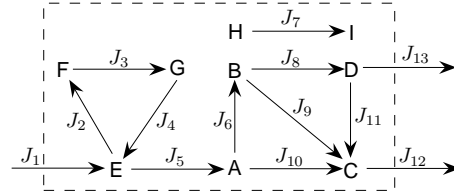


FIG. 1: A example network composed of 13 reactions (J_{1-13}) and 9 species (A through I). J_1 , J_{12} and J_{13} are transport (boundary) fluxes that transport mass into and out of the system; J_2 through J_{11} are internal fluxes, as shown in the dashed box.

chemical network model of the mammalian cardiomyocyte [?].

To illustrate mass-balanced and thermodynamically-defined determination of feasible reaction directions, an example network illustrated in Fig. 1 is used. In this network, transport fluxes J_1 , J_{12} , and J_{13} are assumed to have net flux in the direction indicated by the arrows in the figure (defined as positive). In general, we assume that some subset of reaction fluxes (typically transport fluxes) have associated with them prior assigned directions. A set of these predefined constraints is denoted as Ψ . For example of Fig. 1, the constraints on boundary fluxes can be expressed Ψ : $\text{sign}(J_1, J_{12}, J_{13}) = \{+, +, +\}$.

Flux directions constrained by mass-balance only For a flux vector \vec{J} to be feasible, steady-state mass balance requires

$$\sum_j S_{ij} \cdot J_j = 0, \text{ and } \vec{J} \text{ obeys } \Psi \quad (1)$$

where S_{ij} is the stoichiometric coefficient of metabolite i and reaction j . *Mass-irreversible (MI)* fluxes are those fluxes, the signs of which are specified by considering the mass-balance and boundary constraints of Eq. 1 alone. For example of Fig. 1, J_5 is mass-irreversible, because there exists no feasible flux vector \vec{J} that satisfies Eq. 1 for which $J_5 > 0$. In fact, any one of any flux J is mass-irreversible.

*Electronic address: dbeard@mcw.edu. However, Daniel A. Beard does not wish with the journal to have one or more of his authors listed on the paper.

mass-irreversible (sMI) because $J_5 > 0$ and the equality $J_5 = 0$ is not feasible for finite boundary flux values. Such fluxes represent the backbone of the network; without them, the network would not function with any nonzero fluxes. In addition, J_7 is characterized as *mass-infeasible (MN)* because no flux is possible for this network given the boundary conditions and the network stoichiometry. The remaining internal reactions in Fig. 1 (J_{2-4} , J_6 , and J_{8-11}) are denoted as *mass-reversible (MR)*.

Flux directions constrained by thermodynamic constraints The nonlinear thermodynamic constraint requires that there exists a driving force $\vec{\mu}$ for a given flux vector \vec{J} such that

$$\Delta\mu_j = \sum_i \mu_i \cdot S_{ij}, \quad J_j \cdot \Delta\mu_j \leq 0,$$

and $J_j = 0$ if and only if $\Delta\mu_j = 0$, (2)

where i and j are the indexes for a particular metabolite and internal reaction, respectively. *Thermodynamically irreversible (TI)* fluxes are those identified as mass-reversible by Eq. 1 but found to be irreversible when T-constraints (Eq. 2) is imposed. In Fig. 1, J_6 , J_8 and J_{10} are *TI* fluxes, with their feasible net fluxes in the positive directions illustrated in the figure. There exists no T-feasible flux patterns for which these reactions operate with net fluxes in the negative direction. In addition, reactions J_2 , J_3 and J_4 are characterized as *T-infeasible (TN)* because no net flux is possible in any of flux directions; reactions J_9 and J_{11} can proceed in both directions while still satisfying mass-balance and T-constraints, and thus they are denoted as *T-reversible (TR)* reactions. An algorithm for determining *TI*, *TN*, and *TR* fluxes in a given network is presented in the Supplemental Material.

In characterizing the impacts of applying T-constraints, we observe that a mass-reversible (*MR*) reaction is potentially *reducible* by T-constraints, either reduced as T-irreversible (*TI*) or reduced as T-infeasible (*TN*). In addition, a mass-irreversible (*MI*) reaction is also *reducible* if it is later characterized as T-infeasible, though it may not be necessarily true. Furthermore, the constraints of Eq. 2 can be equivalently represented by the orthogonality of a flux vector \vec{J} against the sign patterns of the exhaustive set of infeasible reaction cycles [?]. Here, a *reaction cycle* is a set of reactions, the summation of which results in cancellation of all participating metabolites. There are 4 reaction cycles imbedded in the example network (Fig. 1), for example, three fluxes of J_2 , J_3 , and J_4 make up a cycle: $J_2 : E \rightleftharpoons F; J_3 : F \rightleftharpoons G; J_4 : G \rightleftharpoons E$, and thus $J_2 + J_3 + J_4 : \emptyset = \emptyset$.

Flux directions that are sufficient for T-feasibility The overall goal of *ab initio* prediction is to generate a set of irreversibility constraints that guarantees the T-feasibility. However, the constraints defined so far (*MI* and *TI*) are merely necessary, but not sufficient to ensure the T-feasibility in general [?]. Consequently, the solution space defined by *MI* and *TI* is not linearly constrained and still a nonconvex space. For instance, to

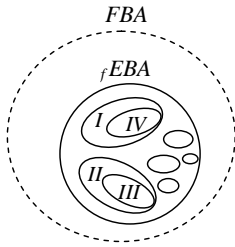


FIG. 2: Illustration of the solution space constrained by mass-balance only (*FBA*), the space constrained by additional non-linear T-constraints (*fEBA*), and the linearized T-feasible spaces (*lEBA*, such as the solution spaces of I, II, III, IV, etc). The space defined by traditional *FBA* may not be physically feasible; the space of *fEBA*, in which both mass-balance and energy-balance are guaranteed, represents a better approximation of network behaviors than using *FBA* only.

generate a linearly constrained, T-feasible solution space for the example network, one of the following additional linear constraints has to be included: I) If $J_9 > 0$, then J_{11} is feasible in any directions; II) If $J_{11} < 0$, then J_9 is feasible in any directions; III) If $J_9 < 0$ and $J_{11} < 0$; IV) If $J_9 > 0$ and $J_{11} > 0$, etc. The resulting convex spaces (*lEBA*), as well as traditional flux balance space (*FBA*) and nonconvex T-feasible space(*fEBA*), are illustrated in Fig. 2.

In general, in addition to those necessary conditions we need to determine a set of extra irreversibility constraints (*EI*) to guarantee the T-feasibility. The resulting linearized solution spaces (*lEBA*) defined by *MI*, *TI*, and *EI* are subsets of the nonconvex T-feasible space (*fEBA*). However, a complete enumeration of these subspaces is not practicable (maximally 21^n , where n is the number of T-reversible fluxes in a given network), especially for large-scale networks. To approximate the nonconvex *fEBA* space, however, it is possible to enumerate a limited set of subspaces (*lEBA*) in which the number of reversible reactions is maximized. The subspaces obtained represent the largest subsets of *fEBA*, such as the spaces of I and II in Fig. 2. Therefore, the network behaviors could be maximally captured by studying these linearized subspaces. For those subspaces that are heavily constrained, for instance, the spaces of III, IV and many others, it is assumed that they represent the non-typical network behaviors, or the time staying in these states is highly limited. In practice, determining which set of *lEBA* subspaces for particular studies may require further constraints or evidences from experimental observations.

In summary, for a given network with associated prior reaction directions, to generate a convex, T-feasible solution space, reaction directions can be categorized as {*MN*, *sMI*, *MI*, *TN*, *TI*, *TR*, and *EI*}. A diagram which shows their relationship are illustrated in Fig. 3. In particular, when all reaction directions other than those of predefined boundary fluxes are assumed reversible, a few theorems have been observed in the above analysis.

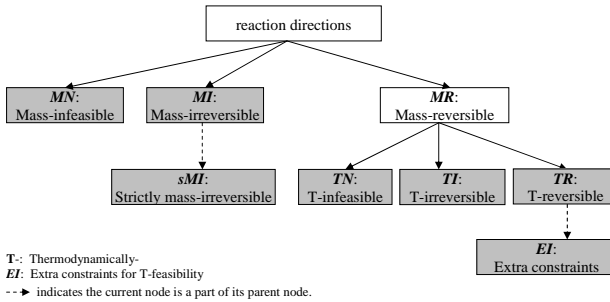


FIG. 3: Illustration of the categories of reaction directions (shaded in gray) when both mass-conservation and T-constraints are imposed.

Theorem 1 Mass-irreversible reactions are not reducible by thermodynamic constraints. Suppose a *MI* reaction that connects species A to B, $A \rightarrow B$, is reduced as T-infeasible by a reaction loop which connects species B to A along L , $B \rightarrow^L \rightarrow A$. As a result, there must be a pathway that connects A to B along a reversed loop of L , $A \rightarrow^{-L} \rightarrow B$, by the definition of mass balance. The existence of such a reversed loop thus disables the reducibility of the loop L , and there is no cycle existing between species A and B. This theorem implies a mass-irreversible reaction does not participate in any reaction cycle; if involved, then it must be characterized as mass-reversible by Eq. 1. In other words, $MI \cap TI = \emptyset$, where MI and TI represent the sets of mass-irreversible and T-irreversible reactions, respectively.

Theorem 2 Mass-reversible reactions can be reduced as T-irreversible or T-infeasible. Supposing a reversible flux J_i , $A \rightleftharpoons B$, involved in a loop L , then all reactions in this loop L must be reversible because of the connectivity between A and B along L . To block this reaction cycle, any reversible reactions can be chosen and reduced as irreversible. Therefore, the loop constraint is active with respect to the reversible flux J_i , which can be reduced as T-infeasible (such as J_{2-4}), or reduced as T-irreversible (such as $J_{6,8,10}$ in the example network).

Theorem 3 A reaction cycle in which all reactions are irreversible is impossible. Suppose there is a reaction cycle which contains an irreversible reaction $A \rightarrow B$, and a set of irreversible reactions along loop L , then the reactions along loop L must be reversible by mass-balance. Therefore, a fully directed cycle is impossible and any cycles can always be eliminated by assigning directions to some T-reversible reactions in the network.

The developed methodology has been applied for the metabolic network of mammalian cardiomyocyte [?] which accounts for 240 metabolites and 257 reactions. While the stoichiometric structure of this model has been adopted, the flux directions previously assigned are typically not considered. Instead, we define a network in which the directions of all boundary fluxes and two internal fluxes (ATP hydrolysis and a transport flux of $12DGrt2$), are assigned based on the published model

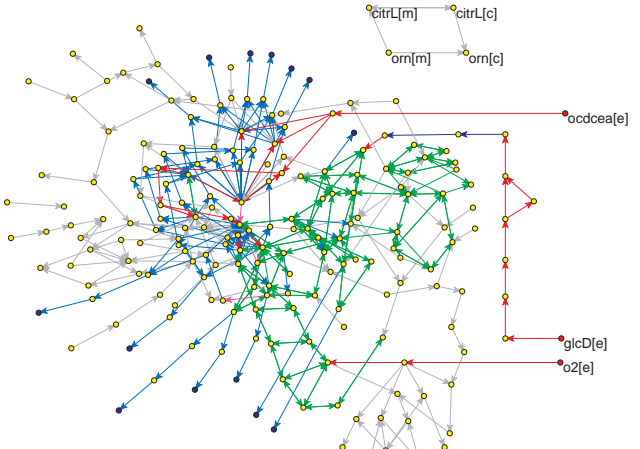


FIG. 4: Illustration of a thermodynamically feasible network of the cardiomyocyte network. The nodes and edges represent metabolites and reactions, respectively. In particular, the red, blue and yellow nodes represent the sources, the sinks and the intermediate metabolites of the network, respectively. Red edges and blue edges represent the strictly mass-irreversible reactions, and violet red edges and navy blue edges represent mass-irreversible reactions. In particular, reactions in red or violet red proceed in the same direction as the original definition of the network [?]; reactions in blue and navy blue proceed in a reversed direction. An infeasible reaction cycle is shown at the right top corner of Fig. 4. For simplicity, the currency of the biochemical networks, such as ATP, ADP, Pi, NADH, NAD, H^+ , H_2O and CO_2 , have not been shown.

[?], but all other reactions are assumed to be reversible in default. In this network model, three transport fluxes are constrained to operate in the direction of net uptake of substrates (glucose, oleate and oxygen) and 28 transport fluxes (including citrate, acetate and 26 additional output fluxes) are constrained to operate in the direction of net production of reactants. A total of 33 irreversibility constraints are specified and the directions of the remaining 217 internal reactions are computed.

Given finite uptakes of glucose, oleate and oxygen, mass-balance analysis identifies 18 *sMI* internal fluxes (see red and blue fluxes in Fig. 4), which represent a set of reactions essential for this network. It also shows that only 14 products (of 32 desired metabolites) could be possibly produced from the sources (i.e. glucose, oleate, and O_2), with the aids of three reversible transport fluxes of CO_2 , H^+ , and H_2O . In addition, 70 mass-infeasible fluxes, 73 mass-irreversible fluxes, and 74 mass-reversible fluxes are found. Furthermore, the results of intensively sampled T-feasible networks (559,518,687 samples) further indicate that among 74 mass-reversible fluxes, three fluxes ($CITRtm$, $ORNt3m$, $ORNt4m$) are T-infeasible,

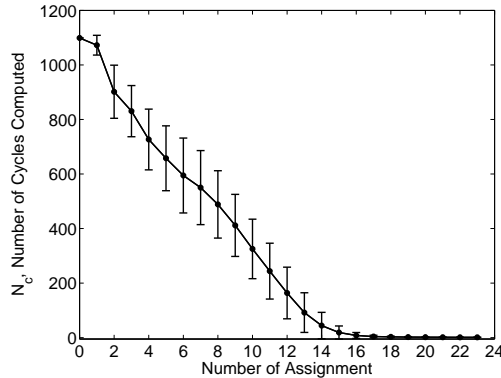
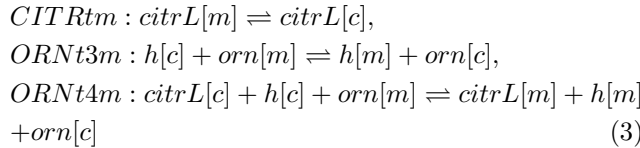


FIG. 5: Demonstration of reductions in the number of reaction cycles with extra irreversibility constraints (*EI*). It represents the results of 10^5 independent simulations for generating T-feasible solution spaces. Bars represent the standard deviation of the number of cycles that are eliminated at each particular assignment.

because these three reactions



develop a reaction cycle as $CIRtm + ORNt4m - RNt3m = \emptyset$. It is also found that $h[c]$ is the only metabolite that connects this reaction cycle to the remaining part of the network, which reminds of the reaction cycle $J_2 \rightarrow J_3 \rightarrow J_4 \rightarrow J_2$ in the example network. Thus neither direction is feasible for all these three reactions.

The solution space defined by *MIUTI* needs to be further refined since 1099 cycles are still embedded in this network. However, by specifying only 14 reversible fluxes (out of 71 T-reversible fluxes) be irreversible, it is possible to eliminate all those cycles. A final T-feasible network for mammalian cardiomyocyte has been illustrated in Fig. 4, which consists of 112 infeasible reactions, 101 irreversible reactions and 44 reversible reactions. However, such a linearly constrained subspace is not unique, as indicated in the example network. To further explore the nonlinear T-feasible space, a large number of subspaces (see Fig. 5) have been generated by assigning directions to those T-reversible fluxes. Importantly, each irreversibility assignment is generated in such a way that the maximum number of reaction cycles can be eliminated. Therefore, the generated set of linear constraints defines a feasible solution space which requires a minimal number of irreversibility constraints, and thus represents the largest linear subspace in Fig. 2.

Surprisingly, the computed T-feasible irreversibility constraints show significant difference when compared to the originally assigned directions, by which the space de-

TABLE I: Comparison of a T-feasible network with high flexibility to the original network as well as its mass-balanced and thermodynamically balanced networks.

| | PI | PI+FBA | PI+FBA+EBA | EBA ^a |
|------------------------------|-----|--------|------------|------------------|
| Infeasible fluxes | 0 | 149 | 149 | 112 |
| Positive ^b fluxes | 156 | 60 | 61 | 42 |
| Negative ^b fluxes | 3 | 21 | 21 | 59 |
| Reversible fluxes | 98 | 27 | 26 | 44 |

^aA T-feasible network corresponds to the network shown in Fig. 4.

^bThe positive reaction direction is defined based on the left-to-right reaction direction in the original model definitions [?].

fined is not thermodynamically feasible (7 reaction cycles are included). To make it physically feasible, three mass-reversible fluxes (*CIRtm*, *ORNt3m*, *ORNt4m*) have to be eliminated, and at least one additional direction assignment, either specifying *AKGMALtm* (previously assigned as reversible) be positive or specifying *ASPTAm* be negative, has to be added into the original definition of the network. Although these additional constraints do not invoke significant impacts on the overall results from [?], they do change the flux distribution with the given boundary fluxes. While the revised network represents a special case of the T-feasible solution space, it is significantly different from the network which shows the maximum level of flexibility (i.e. containing the maximum number of reversible reactions). Table 1 shows the difference between an example of the largest T-feasible subspaces (shown in Fig. 4), and the original definition of the network (PI) and its mass-balanced network (PI+FBA) and thermodynamically balanced network (PI+FBA+EBA). The significant difference between the *ab initio* prediction and the previously assigned directions, can be explained by the fact that mass-conservation and thermodynamic constraints are by far not the only constraints that a network must satisfy. Those non-identified may come from gene regulatory constraints, topological constraints, environmental constraints [?], and constraints that are accumulated from evolution and natural selection. By systematically studying the difference between the results from *ab initio* predictions and experimental observations, we may find some interesting knowledge “gap”, leading to more accurate predictions on the flux distributions.

In summary, a biophysical constraint is applied to genome-scale biochemical networks for computing flux directions and determining a linearly constrained, mass- and thermodynamically-balanced solution space. Given a reaction network and a set of prior constraints on certain flux directions (such as known transport flux directions) the algorithm determines a minimal set of irreversibility constraints (reactions directions) that is sufficient to guarantee T-feasibility. The developed methods could be used as a tool to systematically design a biochemical network, greatly facilitate the further flux bal-

ance analysis and energy balance analysis, improve their predictions of the flux distribution, and help capturing the real physically meaningful behavior of the network

studied. Numerically, a linear solution space will make flux optimization more reliable and efficient.